Proc. of the European Safety and Reliability Conference (ESREL 2026)
Edited by José C. Matos, Paulo B. Lourenço, Michael Beer, Daniel Oliveira,
Edoardo Patelli, Hélder S. Sousa, Rui A. Silva and Monica Santamaria

doi: 10.3850/ESREL2026061419_esrel26-p27830-cd

Robust Design of Electron Beam Welding Process for a Compressor Casing Outer

Lin Han

School of Reliability and Systems Engineering, Beihang University, China. E-mail: hanlin150@buaa.edu.cn

Min Huang

School of Reliability and Systems Engineering, Beihang University, China. E-mail: buaahuang@163.com

Weihan Hu

Basic Technology Department, AECC Hunan Aviation Powerplant Research Institute, China. E-mail: 24966680@qq.com

Guangwei Xia

Basic Technology Department, AECC Hunan Aviation Powerplant Research Institute, China. E-mail: 1073578348@qq.com

Xuejun Liu

School of Reliability and Systems Engineering, Beihang University, China. E-mail: liuxuejun1007@163.com

As a key connecting and load-bearing component of aero-engines, the process quality of the compressor casing directly determines the service life and reliability of the engine. During outer ring electron beam welding, inherent fluctuations in material and equipment parameters easily lead to excessive deformation, crack propagation, and dimensional drift caused by residual stress. Considering parameter uncertainty, this work conducts robust design to reduce welding deformation and residual stress. Firstly, five process parameters are selected to represent the five factors of process reliability (Personnel, Equipment, Materials, Process Methods, Environment). A factorial design is applied to generate simulation schemes, and welding simulations are carried out in SYSWELD to obtain samples of maximum deformation and maximum stress. Secondly, a response surface surrogate model is built via stepwise regression and validated by goodness-of-fit test and analysis of variance. Subsequently, global sensitivity analysis is performed using the Sobol method, and uncertainty quantification is implemented through Monte Carlo sampling with parameter distributions determined by equipment precision and expert experience. Finally, an equal-weight robust optimization model is solved by the particle swarm optimization algorithm. Results show that the optimized scheme significantly reduces the mean values of maximum deformation and stress while suppressing their fluctuations effectively. The proposed framework provides a systematic solution for process improvement of key aero-engine components.

Keywords: SYSWELD, Response Surface Methodology, Robust Design, Compressor Casing Outer.

1. Introduction

The compressor is a core component of aero-engine(Zhao et al. 2022). As the primary load-bearing and connecting component of the compressor, the casing acts as a critical carrier for maintaining structural integrity and airtightness (Nezym 2005). For large-scale casings with complex structures, it is often necessary to assemble multiple components into an integral blank through welding. During the welding process, the uneven heating-cooling cycle induces residual stresses and welding deformations, which may lead to issues such as crack propagation or excessive geometric deviations. In practical production, process parameters typically fluctuate within a certain range due to equipment deviations, and drastic temperature changes also lead to random fluctuations in material parameters, resulting in the uncontrollability of residual stresses and deformations.

In recent years, numerous studies have focused on robust design. (Sameer and Birru 2019) identified the optimal combination of four process parameters using TOPSIS and grey relational analysis. (Lei et al. 2021) compared three robust design methods for low- and high-dimensional optimization and proposed the Space Reduction Optimization strategy to enhance the performance and efficiency of traditional methods. (Chen et al. 2024) implemented distributionally robust optimization for robust design by minimizing the expected worst-case performance in observation-influenced uncertainty distributions, validating it in transonic turbulent aerodynamic shape optimization.

However, most existing studies have neglected the impact of parameter uncertainties, especially in the context of complex welding processes for aero-engine components. Against this backdrop, this paper focuses on the electron beam welding process of the aero-engine compressor casing outer, and considers the influence of the uncertainty of parameters on the residual stress and welding deformation. The structure of this paper is organized as follows: Section 2 introduces the theoretical background; Section 3 establishes the surrogate model of the compressor casing; Section 4 presents the results of sensitivity analysis, uncertainty quantification and robust design based on the surrogate model; and Section 5 draws conclusion.

2. Method

This study is mainly consists of three stages. Firstly, based on the SYSWELD software, a numerical simulation model for the electron beam welding process of the compressor casing outer ring is established through mesh generation, material definition, boundary condition setting and constraint definition to predict the residual stress and welding deformation. Secondly, process parameters are identified to implement factorial design. Simulation calculations are conducted according to the experimental scheme to acquire sample data, and a response surface surrogate model is built. Global sensitivity analysis is subsequently performed using the Sobol variance decomposition method. Finally, uncertainty quantification of process parameters is performed via Monte Carlo simulation. A robust design approach is employed to minimize residual stress and deformation, finding the optimal parameter combination that balances quality and reliability.

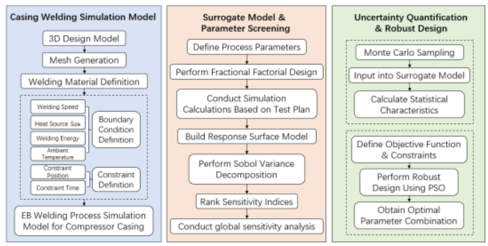

Fig. 1.Technical roadmap for research

2.1.*Response surface methodology*

Response surface methodology (RSM) is a classic surrogate model approach based on polynomial regression. Its core idea is to approximate the nonlinear relationship between input parameters and output responses with low-order polynomials. The response surface model is based on polynomial regression theory, assuming an explicit polynomial relationship between the system response y and input parameters $\boldsymbol{x} = (x_1, x_2, \dots, x_k)$. The commonly used second-order model is expressed as follows:

$$y = \beta_0 + \sum_{i=1}^{k} \beta_i x_i + \sum_{i=1}^{k} \beta_{ii} x_i^2 + \sum_{i<j}^{k} \beta_{ij} x_i x_j + \varepsilon \quad (1)$$

where β_0 is the constant term; $\beta_i, \beta_{ii}, \beta_{ij}$ represent the coefficients of linear terms, quadratic terms, and interaction terms; and ε denotes the random error term.

2.2.*Sobol sensitivity analysis method*

Assume the model output is $Y = f(\mathbf{X})$, where $\mathbf{X} = (X_1, X_2, \dots, X_k)$ denotes the input parameters. According to Sobol decomposition theory, the model can be expressed as follows:

$$Y = f_0 + \sum_{i=1}^{k} f_i(X_i) + \sum_{1 \le i < j \le k} f_{ij}(X_i, X_j) + \cdots + f_{12\dots k}(\mathbf{X}) \quad (2)$$

Through orthogonality conditions, the total variance can be decomposed as follows:

$$\mathrm{Var}(Y) = \sum_{i=1}^{k} V_i + \sum_{1\le i<j\le k} V_{ij} + \cdots + V_{12\ldots k} \quad (3)$$

Accordingly, the first-order Sobol index S_i is defined as follows:

$$S_i = \frac{V_i}{\mathrm{Var}(Y)} = \frac{\mathrm{Var}(E[Y|X_i])}{\mathrm{Var}(Y)} \quad (4)$$

The total-effect index ST_i is given as follows:

$$S_{Ti} = \frac{V_i + \sum_{j\ne i} V_{ij} + \cdots + V_{12\ldots k}}{\mathrm{Var}(Y)} = 1 - \frac{\mathrm{Var}(E[Y|X_{\sim i}])}{\mathrm{Var}(Y)} \quad (5)$$

2.3. *Uncertainty quantification*

Monte Carlo method is the mainly uncertainty quantification method (Helton et al. 2006).First, define the probability distribution of each input parameter to represent its uncertainty, i.e., $\boldsymbol{x} \sim H$. Then, multiple independent samples x_i are drawn from the uncertainty distribution of the input parameters and substituted into a model for deterministic computation to obtain the results $f(\boldsymbol{x}_i) = y_i$. Finally, the characteristics of the output data distribution are statistically analyzed; commonly used metrics include the mean $\bar{y}$ and variance σ_y^2, as shown in Eq. (6) and Eq. (7) respectively (Price et al. 2022).

$$\bar{y} = \frac{1}{N}\sum_{i=1}^{N} y_i \quad (6)$$

$$\sigma_y^2 = \frac{1}{N}\sum_{i=1}^{N} (y_i - \bar{y})^2 \quad (7)$$

2.4. *Robust Design*

Robust Design (RD) is a methodology that focusing on optimizing system performance while controlling the fluctuation of uncertain parameter(Bidoki et al. 2019). The minimax method is a commonly RD approach: it establishes a RD model while adopting a weighted combination of the mean values and standard deviations of output parameters as the objective function, and takes the value ranges of input parameters as constraint conditions.

$$\begin{cases} \min Objective \\ s.t. P_c^{LB} \le P_c \le P_c^{UB}, c = 1,2,\cdots,N \end{cases} \quad (8)$$

where P_c represents the c-th parameter, P_c^{UB}, P_c^{LB} are the upper and lower bounds of P_c respectively, and N is the number of parameters.

For the smaller-the-better response index $Y(Y \ge 0)$, its objective function can be expressed as follows:

$$Objective = \omega_1 \frac{\mu_Y}{\mu_0} + \omega_2 \frac{\sigma_Y}{\sigma_0} \quad (9)$$

where μ_Y denotes the mean value of the response parameter, σ_Y represents the standard deviation of the response parameter, μ_0 is the initial mean value of the response parameter, σ_0 is the initial standard deviation of the response parameter, ω_1, ω_2 are weight coefficients satisfying $\omega_1 + \omega_2 = 1$.

The robust design of output responses satisfying input parameter constraints is a constrained optimization problem. Two types of methods are available for solving such optimization problems: gradient-based methods and metaheuristic methods(Nouri and Valadi 2017). Particle Swarm Optimization (PSO) is an excellent gradient-based methods, which reduces the requirements for continuous cost functions and variables and does not require the derivatives of cost functions and constraints(Garg 2016).

3. Welding Process Simulation Model

3.1. *Introduction to a Compressor Casing*

The compressor casing is a core component of aero-engine. Its main structure comprises an outer shell that houses the compressor rotor and stator, typically featuring an annular configuration with longitudinal mounting flanges, as shown in Fig. 2.

Fig. 2.Schematic diagram of compressor casing

3.2. *Establishment of the process simulation model for a compressor casing outer ring*

3.1.1. *Mesh generation*

Based on the 3D design model of the casing outer ring, hexahedral elements were adopted to generate 3D meshes through rotational sweeping, with the element size ranging from $1mm \le h_{elem} \le 3mm$. The mesh was refined to ensure at least three layers of elements in this region.

Fig. 3.3D design model and process simulation model

3.1.2. *Definition of boundary conditions*

Parameters including welding speed, welding energy and ambient temperature were set according to the actual working conditions during component welding.

A Gaussian heat source was used to represent the welding heat input, where the top diameter, bottom diameter and penetration depth were set to be no less than the measured dimensions of the loading area near the weld, and other relevant parameters are listed in Table 1..

The constraint positions were consistent with the fixture locations employed in the actual welding process of the component.

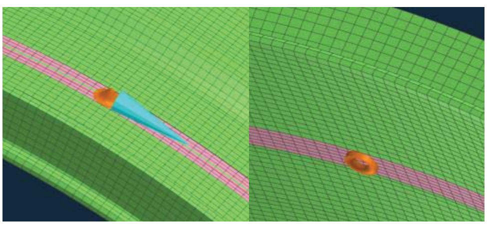

Fig. 4.Schematic diagram of the heat source

Table 2. Process parameters

Parameter	Setting
Welding Speed	20mm/sec
Top Diameter	8mm
Bottom Diameter	6mm
Penetration Depth	7mm
Accelerating Voltage	120kV
Beam Current	26mA
Energy per Unit Length	156J/mm
Welding Efficiency	0.8
Ambient Temperature	20℃
Total Cooling Time	1500s
Rigid Clamp Time	1200s
Unclamp Time	300s

4. Results

4.1.*Establishment of response surface model*

4.1.1.*Input and output parameters*

To characterize the five elements of process reliability analysis (personnel, equipment, materials, process methods, and environment), five adjustable parameters in SYSWELD—thermal conductivity (x_1), penetration depth (x_2), ambient temperature (x_3), welding energy (x_4), and cooling time (x_5)—were selected as the input parameters of the response surface model. It should be noted that, in this study, x_2 represents the preset target value of the molten pool depth in the heat source model, which can be directly set and adjusted in the SYSWELD welding simulation software.The model was constructed with maximum deformation ($Y1$) and maximum stress ($Y2$) as the output process indicators.

4.1.2.*Sample acquisition*

A factorial design was adopted to investigate the influence law of input parameters on process indicators. A two-level coding scheme was used to represent the low and high levels of each factor. Simulation calculations are performed according to the experimental scheme, yielding 23 sets of valid samples (Table 3).

Table 3. Sample data

No	x_1	x_2	x_3	x_4	x_5	$Y1$	$Y2$
1	-1	-1	-1	-1	-1	0.15285	685.19
2	1	-1	-1	-1	1	0.13965	679.52
3	-1	1	-1	-1	1	0.14907	677.08
4	1	1	-1	-1	-1	0.14048	674.44
5	-1	-1	1	-1	1	0.16185	693.40
6	1	-1	1	-1	-1	0.12415	696.23
7	-1	1	1	-1	-1	0.13326	694.33
8	1	1	1	-1	1	0.12724	681.89
9	-1	-1	-1	1	1	0.19769	800.11
10	1	-1	-1	1	-1	0.19053	831.88
11	-1	1	-1	1	-1	0.18801	986.42
12	1	1	-1	1	1	0.22446	944.08
13	-1	-1	1	1	-1	0.17849	1040.7
14	1	-1	1	1	1	0.17384	1001.6
15	-1	1	1	1	1	0.18338	995.01
16	1	1	1	1	-1	0.17950	1030.1
17	-1	0	0	0	0	0.17192	694.40
18	1	0	0	0	0	0.17357	681.84
19	0	-1	0	0	0	0.17898	686.27
20	0	1	0	0	0	0.17196	677.01
21	0	0	-1	0	0	0.16547	682.51
22	0	0	0	0	1	0.17096	695.11
23	0	0	0	0	0	0.17082	694.95

4.1.3.*Maximum deformation*

Variables are screened by stepwise regression method, and a second-order response surface model for maximum deformation is constructed. The overall fitting performance of the model is presented in Table 4.

Table 4. Model fitting metrics

S	R-sq	R-sq(Adjusted)
0.0036357	99.06%	97.70%

The coefficient of determination of the model reached 99.06%, and the adjusted coefficient of determination was 97.70%, indicating that the model can explain 97.70% of the variation in maximum deformation, with only 2.3% of the variation attributed to random errors. This demonstrates the strong explanatory power of the model for the data.

Table 5. Analysis of Variance Table

Source of Variation	df	Adj-SS	F-value	P-value
Model	13	0.0125	73.001	0.0000
Linear	5	0.0106	161.000	0.0000
x_1	1	0.0001	7.809	0.0209
x_2	1	0.0000	0.002	0.9664
x_3	1	0.0008	63.392	0.0000
x_4	1	0.0094	709.450	0.0000
x_5	1	0.0003	24.144	0.0008
x_2^2	1	0.0001	5.067	0.0509
x_3^2	1	0.0003	20.126	0.0015
x_1x_2	1	0.0004	30.767	0.0004
x_1x_3	1	0.0002	16.883	0.0026
x_1x_4	1	0.0005	35.204	0.0002
x_2x_3	1	0.0001	6.213	0.0343
x_2x_4	1	0.0002	18.909	0.0019
x_3x_4	1	0.0002	11.790	0.0075
Square+ Inter	8	0.0002	18.003	0.0001
Error	9	0.0001	0.0000	
Total	22	0.0127		

As shown in Table 5, the overall P-value of the model is close to 0.0000, and the F-test is highly significant, indicating that the response surface model has a strong explanatory ability for the maximum deformation. The first-order terms are highly significant as a whole, among which x_4(Adj-SS = 0.0094) exerts the greatest influence. The P-value of the quadratic and interaction terms is 0.0001, which demonstrates the existence of significant nonlinear effects in the model, and the interaction term x_1x_4 contributes the most.

4.1.4.*Maximum stress*

Similarly, the response surface model for maximum stress is established by the stepwise regression method. The overall fitting performance and analysis of variance of the model are presented in Table 6 and Table 7.

Table 6. Model fitting metrics

S	R-sq	R-sq(Adjusted)
10.9784606	99.72%	99.38%

Table 7. Analysis of Variance Table

Source of Variation	df	Adj-SS	F-value	P-value
Model	12	429867.0958	297.215	0.0000
Linear	5	320561.0878	531.934	0.0000
x_1	1	112.9204	0.937	0.3559
x_2	1	3346.0290	27.762	0.0004
x_3	1	25020.2407	207.591	0.0000
x_4	1	288323.6253	2392.199	0.0000
x_5	1	3708.6838	30.771	0.0002
x_3^2	1	67288.0926	558.284	0.0000
x_4^2	1	84922.1247	704.592	0.0000
x_1x_5	1	6222.1727	51.625	0.0000
x_2x_3	1	6239.5386	51.769	0.0000
x_2x_4	1	5923.8036	49.149	0.0000
x_3x_4	1	12956.5290	107.499	0.0000
x_4x_5	1	1055.9413	8.761	0.0143
Square+ Inter	7	109306.0080	129.558	0.0000
Error	10	1205.2660		
Total	22	431072.3618		

4.2.*Global sensitivity analysis*

The Sobol variance decomposition method was used to quantify the contribution of input parameters to the outputs of maximum deformation and maximum stress, clarifying the individual contribution, total contribution, and interaction characteristics of each parameter.

4.2.1.*Maximum deformation*

As shown in Fig. 5, ambient temperature is the core control parameter for maximum deformation. Its first-order sensitivity index (S) is as high as 0.9431, and the total effect index S_T is 0.9526, contributing more than 95% of the total variance. Welding energy is the secondary influencing parameter, accounting for approximately 4% of the total variance. In contrast, thermal conductivity, penetration depth and cooling time have virtually no substantial impact on maximum deformation.

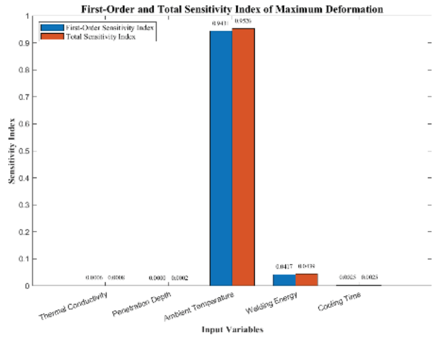

Fig. 5.Comparison chart of sensitivity indices for maximum deformation

4.2.2.*Maximum stress*

As illustrated in Fig. 6, ambient temperature is the core control parameter for maximum stress. Its sensitivity index S is 0.9112 and the total effect index S_T is 0.9114. The difference between S_T and S is only 0.0002, indicating that the independent effect of this parameter is absolutely dominant, and its interaction with other parameters is extremely weak. Welding energy accounts for approximately 9% of the total variance and serves as a secondary influencing factor. In contrast, the effects of thermal conductivity, penetration depth and cooling time are negligible.

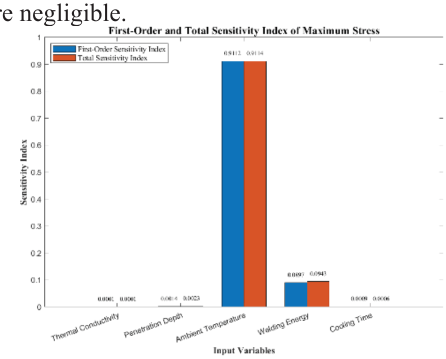

Fig. 6.Comparison chart of sensitivity indices for maximum stress

4.3.*Uncertainty quantification(UQ)*

The normal distribution of cooling temperature is fitted based on the 2024 temperature data of the equipment location to determine its mean and standard deviation. For the remaining parameters, the mean values of their normal distributions are set according to the actual welding process parameters of the components, while the standard deviations are comprehensively determined based on equipment accuracy and engineering experience. The specific variation ranges are presented in Table 8. A total of 10^6 Monte Carlo samplings are performed on the input parameters, and the statistical characteristics of the output indicators are calculated by the surrogate model.

Table 8. Fluctuation characteristics of input parameters

	x_1	x_2	x_3	x_4	x_5
Mean	1(base line)	7	20.7	156	1200
Std.	0.01	0.066 67	5.59	0.78	20

4.3.1.*Maximum deformation*

As shown in Table 9 and Fig. 7, the coefficient of variation of the maximum deformation is 3.41 %, and the width of the 95% confidence interval is 0.0214 mm. The relative deviations between extreme values and the mean are all less than 7 %, indicating favorable overall stability. The uncertainty distribution of the maximum deformation presents a bimodal skewed distribution. The primary peak concentrates in the range of 0.167–0.172 mm, while the secondary peak appears around 0.152 mm. This phenomenon reveals that quadratic terms and interaction effects lead to the formation of two stable states.

Table 9. UQ table for maximum deformation

Mean	Std.	CV	95% Confidence Interval	Min~Max
0.1669	0.0057	3.41%	[0.1519, 0.1733]	0.1467~0.1775

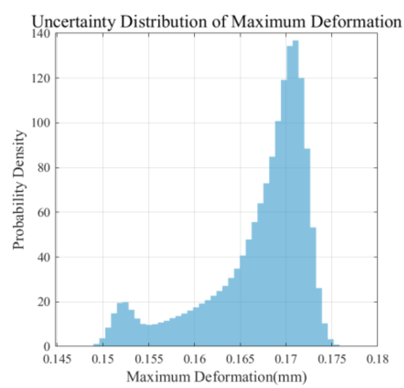

Fig. 7.UQ Distribution chart of maximum deformation

4.3.2. *Maximum stress*

As shown in Table 10 and Fig. 8, the 95% confidence interval width of the maximum residual stress reaches 81.78 MPa, and the global maximum value is 13.5% higher than the mean value, indicating that the stress may rise under extreme operating conditions. The uncertainty distribution of the maximum residual stress exhibits a right-skewed characteristic. The main peak corresponds to the stable stress level under most working conditions, while the long tail on the right side corresponds to a small number of high-stress conditions. This indicates that the combination of high welding energy and low cooling efficiency will cause a significant increase in residual stress, leading to potential process risks.

Table 10. UQ table for maximum stress

Mean	Std.	CV	95% Confidence Interval	Min~Max
699.8742	22.2009	3.17%	[672.17, 753.95]	656.4~794.5

4.4. *Robust Design*

Since ambient temperature of welding equipment cannot be artificially controlled, the ambient temperature parameter is fixed at the average temperature of the equipment location in 2024. Only four parameters are optimized, including thermal conductivity, penetration depth, energy input and cooling time. The objective function is formulated to minimize the sum of the mean and standard deviation of maximum deformation and maximum residual stress. The optimal combination of process parameters is obtained by the PSO algorithm, as shown in Table 11.

Table 11. Optimal parameter combination table

x_1	x_2(mm)	x_3(℃)	x_4(J/mm)	x_5(s)	$Y1$		$Y2$	
					Mean(mm)	Std.	Mean(MPa)	Std.
0.9700	6.8000	20.7	153.6600	1260.000	0.1652	0.0051	677.9792	21.5885

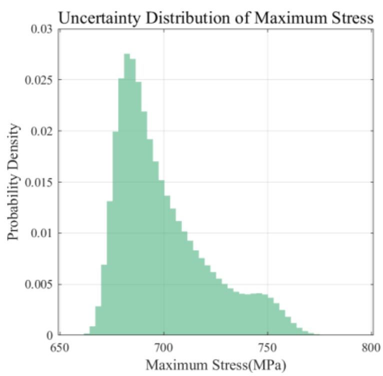

Fig. 8.UQ distribution chart of maximum stress

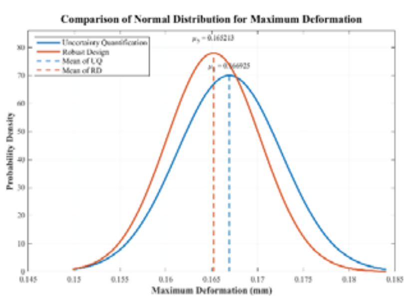

(a) Maximum deformation

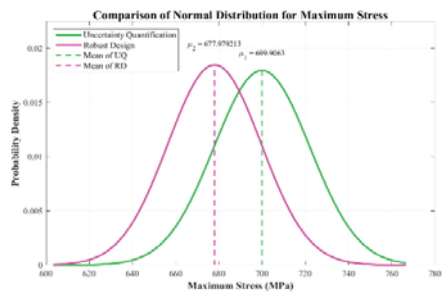

(b) Maximum stress

Fig. 9.Comparison chart of robust design and UQ

As illustrated in Fig. 9, with respect to the maximum deformation, the distribution curve after robust design shifts toward lower deformation values compared with the original uncertainty results, accompanied by a more concentrated distribution and a higher peak. This indicates that both the mean value and dispersion degree of deformation are effectively improved. For the maximum residual stress, robust design also achieves significant improvements. The corresponding distribution curve is markedly narrowed, and the long tail extending toward high stress values is substantially reduced, which effectively suppresses the risks under extreme operating conditions. Overall, the proposed robust optimization strategy simultaneously reduces the mean values and restrains the fluctuation levels of both deformation and residual stress. It not only improves the overall welding quality but also mitigates the uncertainty caused by parameter variations, thereby effectively eliminating potential extreme risks in the welding process.

5. Conclusion

In this study, a process simulation model was established for the electron beam welding of the aero-engine compressor outer ring. Sample data of maximum deformation and maximum stress were acquired through numerical simulation, based on which a response surface surrogate model was established. Global sensitivity analysis and uncertainty quantification were subsequently performed using this surrogate model, and a robust design framework accounting for parameter variability was proposed. The results demonstrate that the optimal parameter combination significantly reduces the mean values of maximum deformation and maximum stress while effectively controlling their fluctuations. Although this study has achieved the intended research objectives, it still has certain limitations, primarily manifested in the consistency issue between numerical simulation results and physical test data. To address this, future research will conduct in-depth exploration in the field of model calibration and further enhance the accuracy of the simulation model by integrating physical experiments.

References

Bidoki M, Mortazavi M, Sabzehparvar M (2019) A new multidisciplinary robust design optimization framework for an autonomous underwater vehicle in system and tactic design. Proceedings of the Institution of Mechanical Engineers, Part M: Journal of Engineering for the Maritime Environment 233:918–936. https://doi.org/10.1177/1475090218791081

Chen L, Rottmayer J, Kusch L, et al (2024) Data-driven aerodynamic shape design with distributionally robust optimization approaches. Computer Methods in Applied Mechanics and Engineering 429:117131. https://doi.org/10.1016/j.cma.2024.117131

Garg H (2016) A hybrid PSO-GA algorithm for constrained optimization problems. Applied Mathematics and Computation 274:292–305. https://doi.org/10.1016/j.amc.2015.11.001

Helton JC, Johnson JD, Sallaberry CJ, Storlie CB (2006) Survey of sampling-based methods for uncertainty and sensitivity analysis. Reliability Engineering & System Safety 91:1175–1209. https://doi.org/10.1016/j.ress.2005.11.017

Lei G, Bramerdorfer G, Liu C, et al (2021) Robust Design Optimization of Electrical Machines: A Comparative Study and Space Reduction Strategy. IEEE Trans Energy Convers 36:300–313. https://doi.org/10.1109/TEC.2020.2999482

Nezym V (2005) Parametric investigation of entire annular recess casing treatment on compressor stable operation. Experimental Thermal and Fluid Science 29:209–215. https://doi.org/10.1016/j.expthermflusci.2004.04.002

Nouri NM, Valadi M (2017) Robust input design for nonlinear dynamic modeling of AUV. ISA Transactions 70:288–297. https://doi.org/10.1016/j.isatra.2017.02.006

Price D, Maile A, Peterson-Droogh J, Blight D (2022) A methodology for uncertainty quantification and sensitivity analysis for responses subject to Monte Carlo uncertainty with application to fuel plate characteristics in the ATRC. Nuclear Engineering and Technology 54:790–802. https://doi.org/10.1016/j.net.2021.09.010

Sameer MD, Birru AK (2019) Optimization and characterization of dissimilar friction stir welded DP600 dual phase steel and AA6082-T6 aluminium alloy sheets using TOPSIS and grey relational analysis. Mater Res Express 6:056542. https://doi.org/10.1088/2053-1591/aafba4

Zhao B, Zhou T, Yang C (2022) Experimental investigations on effects of the self-circulation casing treatment on acoustic and surge characteristics in a centrifugal compressor. Aerospace Science and Technology 131:108002. https://doi.org/10.1016/j.ast.2022.108002